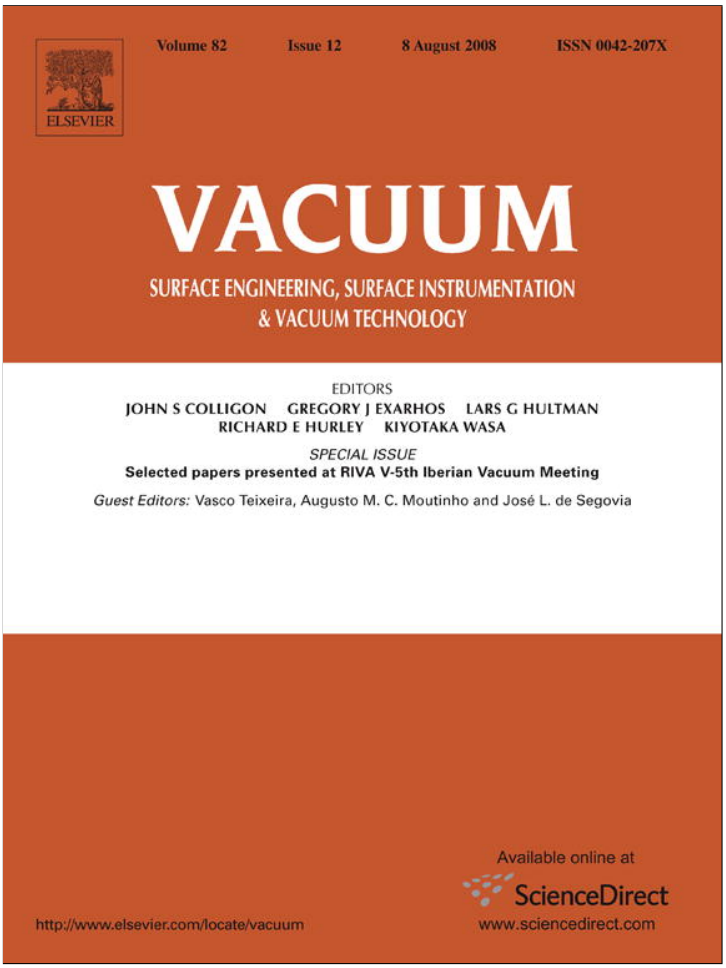

Vacuum 82 (2008) 1395–1399

Contents lists available at ScienceDirect

Vacuum

journal homepage: www.elsevier.com/locate/vacuum

Branched structures of tin oxide one-dimensional nanomaterials

Hyoun Woo Kim*, Seung Hyun Shim

School of Materials Science and Engineering, Inha University, Incheon 402-751, Republic of Korea

Keywords:
SnO_2
Nanomaterials
Thermal evaporation
Branched structures

A B S T R A C T

Branched structures of SnO_2 one-dimensional nanomaterials have been successfully fabricated via a novel multi-step process. Scanning electron microscopy indicated that the SnO_2 branches, which sprouted from the SnO_2 stems, had diameters in the range of 30–120 nm. X-ray diffraction, high resolution transmission electron microscopy and selected area diffraction pattern revealed that the branches were single crystalline rutile SnO_2 structures. Room temperature photoluminescence spectrum of the branched product exhibited visible light emission. We suggested that a Au-catalyzed vapor–liquid–solid growth mechanism was responsible for the growth of SnO_2 branches on the SnO_2 stems.

1. Introduction

Tin oxide (SnO_2) is a key functional material which has multi-faceted technological applications including optoelectronic devices [1,2] and gas sensors [3–6]. In addition, SnO_2 is regarded as one of the most promising materials for dye-based solar cells, transparent conducting electrodes, and catalyst supports. Since one-dimensional (1D) nanostructures including nanowires, nanorods, and nanoribbons, have great potential due to their novel physical properties and industrial applications in nanodevices, the synthesis of SnO_2 1D nanomaterials has been intensively studied [7–11]. Furthermore, one of the most interesting and urgent challenges is the fabrication of 1D material with a novel morphology. In particular, branched 1D nanomaterials offer another approach for increasing structural complexity and enabling greater function [12]. The fabrication of branched nanostructures will enable not only to connect the nanorods of different characteristics including diameter, but also to enlarge the surface-to-volume ratio, contributing to the potential applications to future nanoelectronics and nanodevices. Up to the present, the branched carbon nanotubes have been synthesized by different methods in many research groups [13–15], whereas not many works have been reported on the branched inorganic nanomaterials.

In the present work, we have successfully grown the SnO_2 branches on the SnO_2 1D nanostructures by a novel technique, in which we have pre-deposited the thin Au layers on the surface of SnO_2 1D stems and subsequently heated using the conventional furnace. In addition, we have investigated structural and photoluminescence (PL) properties.

2. Experimental

First, 1D nanostructures of SnO_2 have been prepared by evaporating Sn powders [16]. The sketch of the used apparatus is previously reported [17]. The gold (Au)-coated Si substrate was put on top of an alumina boat loaded with the pure Sn powders. The alumina boat was put in the middle of quartz tube inserted in a horizontal tube furnace. During the experiment, the furnace was maintained at a temperature of 1173 K under a constant total gas pressure of 1 Torr for 2 h. After the furnace was cooled down, the sample was removed from the furnace and then was transferred to a sputtering chamber (Emitech, K757X), in which Au films of about 2.5 nm thick were deposited on the SnO_2 1D nanostructures. After Au deposition, samples were annealed for 20 min at 973 K in N_2 ambient.

Subsequently, we have carried out the branch-growing experiments on the SnO_2 1D nanostructure stems. The schematic diagram of the heating system is previously reported [18]. The SnO_2-grown substrate was placed on the upper holder in the furnace. During the experiment, a constant flow of nitrogen (N_2) was maintained at flow rate of 500 sccm. The temperature near the substrate was about 1173 K for 2 h. After evaporation, the substrate was cooled down and subsequently taken out from the furnace for structural and optical characterization.

The structural properties of the products were investigated using grazing angle X-ray diffraction (XRD: Cu$K\alpha_1$ radiation) (Philips X'pert MRD) with an incidence angle of 0.5°, field emission scanning electron microscopy (FE-SEM) (Hitachi, S-4200), transmission electron microscopy (TEM) (Philips, CM-200), and energy dispersive X-ray spectroscopy (EDX). For TEM observation, the products were ultrasonically dispersed in acetone, and then a drop of the suspension was placed on amorphous carbon films supported by copper grids and dried in air. PL measurement was conducted at

* Corresponding author.
E-mail address: hwkim@inha.ac.kr (H.W. Kim).

0042-207X/$ – see front matter © 2008 Elsevier Ltd. All rights reserved.
doi:10.1016/j.vacuum.2008.03.074

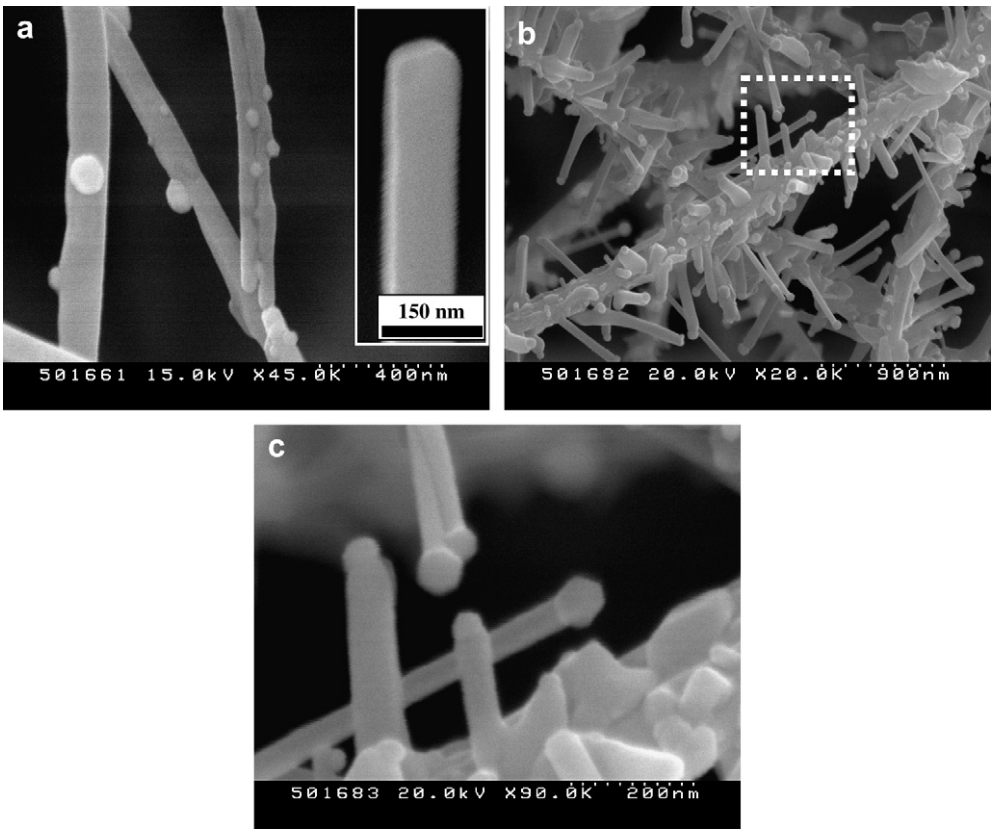

Fig. 1. SEM images of the products (a) after the Au films were deposited and annealed (right inset: SEM image of a SnO_2 nanorod prior to Au deposition) and (b) after the branches have been grown. (c) High magnification SEM image enlarging a boxed area in Fig. 1b.

room temperature with the 325 nm line from a He–Cd laser (Kimon, 1 K, Japan).

3. Results and discussion

Fig. 1a shows a typical SEM image of the SnO_2 1D nanostructure stems, after the Au films were deposited and annealed, revealing that there exist some nanoparticles on the surface of the SnO_2 1D structures. On the contrary, we do not observe any nanoparticle on the surface of the as-synthesized SnO_2 1D structures prior to Au deposition (right inset in Fig. 1a) or on the surface of the Au-deposited SnO_2 1D structures prior to annealing (not shown here). Therefore, we surmise that the nanoparticles have been formed by agglomeration of pre-deposited Au films during the annealing treatment. Fig. 1b shows the SEM image of the branched SnO_2 1D nanostructures. As shown in Fig. 1b, the product consists of branched structures, which displays numerous characteristic branches attached to main stems. Statistical observation of many SEM images indicates that the average diameter and length of the SnO_2 branches are in the range of 30–120 nm and up to 1 μm, respectively. Fig. 1c shows the high magnification SEM image, indicating that the diameter of each branch is almost uniform from the bottom to the top, terminating at a nanoparticle at the tip.

Fig. 2 shows the typical XRD pattern of the branched product. The XRD peaks can be indexed based on a tetragonal cell (rutile structure) with cell parameters $a = 0.473$ nm and $c = 0.318$ nm, which is in good agreement with the known data (JCPDS Card File No. 41-1445). The strong and sharp reflection peaks suggest that the as-synthesized products are well crystallized. Although Au-related peaks are not clearly observed in this spectrum, it is possible that some Au-related peaks are overlapped with SnO_2 peaks. In our XRD measurements, the angle of the incident beam to the substrate surface was about 0.5°, and a detector rotated to scan the samples. Therefore, we surmise that the peaks are mainly from the product. It is noteworthy that there exist very weak peaks, which can be indexed to (200) and (101) reflection of tetragonal structure of Sn with lattice constants of $a = 5.831$ Å and $c = 3.182$ Å (JCPDS File No. 04-0673). Although the Sn-related peaks are considered to be originated from unreacted Sn powders, there is a possibility that Sn could be generated during the synthetic process as a result of the reaction: $2SnO = SnO_2 + Sn$ [19].

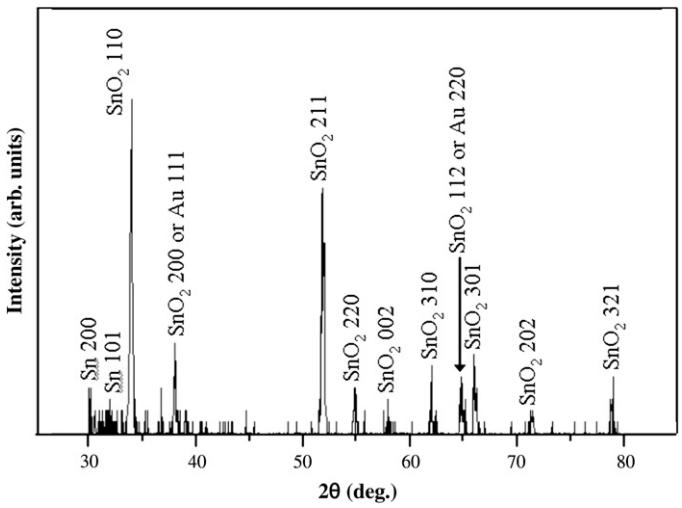

Fig. 2. XRD pattern of the product.

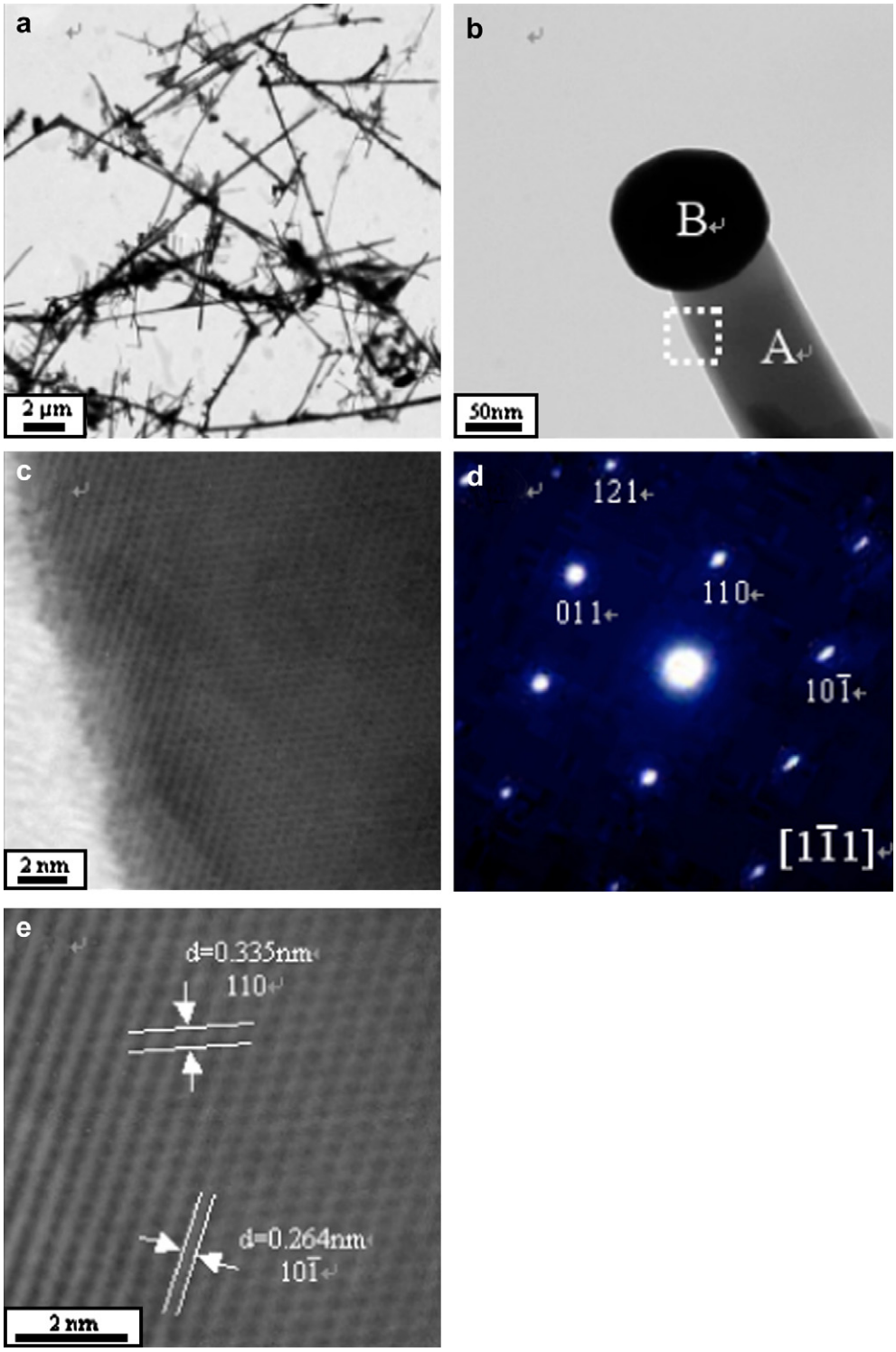

Fig. 3. (a) Low-magnification TEM image of the product. (b) TEM image of a single branch. (c) HRTEM image taken at the area marked with the rectangular box in (b) and (d) associated SAED pattern. (e) Lattice-resolved HRTEM image.

Fig. 3a shows the low-magnification TEM image, revealing the branched morphology of SnO_2 1D nanostructures. Fig. 3b shows a TEM image of a single branch. The nanoparticle at the tip of the branch appears dark and has high contrast compared with the branch part. Fig. 3c is a high resolution TEM (HRTEM) image taken at the area marked with the rectangular box in Fig. 3b, indicating that the branch is structurally uniform with an almost smooth surface. The corresponding selected area electron diffraction (SAED) pattern (Fig. 3d) can be indexed to be [1 $\bar{1}$ 1] zone axis of the rutile structured SnO_2 crystal, revealing the single crystalline nature of the branches. A lattice-resolved HRTEM image taken near the edge along this branch is shown in Fig. 3e. The interplanar spacings are approximately 0.264 and 0.335 nm, corresponding to the (1 0 $\bar{1}$) and (110) plane of rutile SnO_2. Fig. 4a and b shows the EDX spectra associated with spot A and spot B in Fig. 3b, respectively. The C and Cu components have originated from the C-

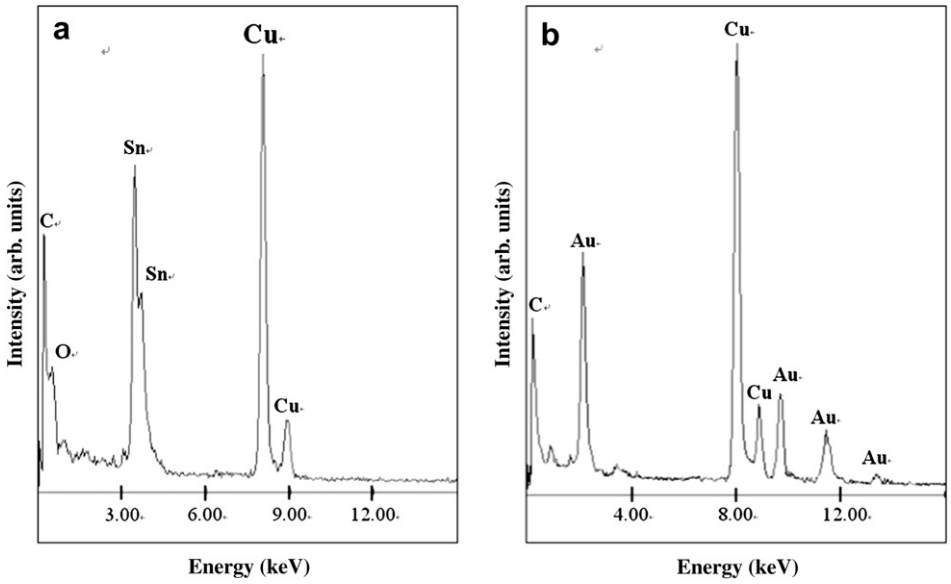

Fig. 4. EDX spectra of (a) the branch (spot A in Fig. 3b) and (b) the tip (spot B in Fig. 3b).

coated Cu TEM grid. Apart from C and Cu, while the EDX pattern of the branch (spot A) shows elemental Sn and O, that of the tip (spot B) shows elemental Au.

There are two well-accepted mechanisms for the growth of 1D nanostructures; the vapor–liquid–solid (VLS) and the vapor–solid (VS) mechanism. The VLS growth is a catalyst-assisted process, in which the metal catalyst particle acts as liquid-forming agent. In the present work, SEM images, TEM images, and EDX measurements coincidentally indicate that the branch tips comprise metal particles. Hence, VLS mechanism may be more valid than the VS one to demonstrate the growth of SnO_2 branches in the present synthesis route. We surmise that the Au film deposited on SnO_2 stems agglomerate during the subsequent annealing step, forming the nanoparticles as shown in Fig. 1a. These nanoparicles, which mainly consist of Au, will function as a catalyst for the VLS growth of SnO_2 branches in the following heating step. It is believed that the oxygen in the SnO_2 branches has been originally come from the air leakage or the residual oxygen in the furnace. Although we have used a N_2 atmosphere during the heating process in the furnace, there should exist the air leakage or the residual oxygen in the N_2 flow. Also, since Sn or Sn-related powders were not intentionally introduced during the branch-growing step, we surmise that the Sn in the SnO_2 branches has been originally come from the unreacted Sn or other tin oxides in the pre-grown product which comprises SnO_2 stems. Further systematic study is necessary in order to reveal the detailed mechanism.

Fig. 5 shows a room temperature PL spectrum of the branched product. There is an apparent broad emission PL band, which can be a superimposition of several peaks. The dominant emission peak is located at a wavelength around 610 nm, corresponding to the energy of about 2.04 eV in the yellow region. The yellow luminescence is known to be associated with defect energy levels within the band gap of SnO_2 [20,21]. It is noteworthy that there exists a blue emission shoulder around 420–450 nm. Similar blue emission has been observed from sintered tin oxide, being related to defects [22]. This result will contribute to the potential applications of branched 1D nanostructures to optoelectronic devices.

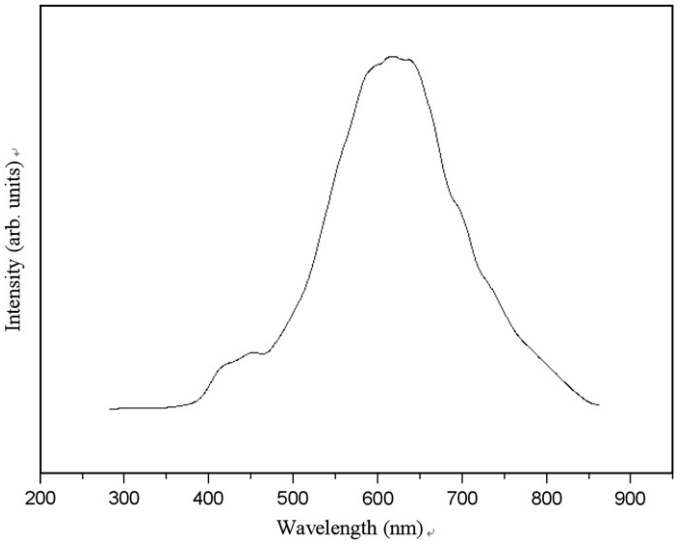

Fig. 5. Room temperature PL spectrum of the product.

4. Conclusions

An approach to the growth of branched SnO_2 nanostructures has been reported, in which SnO_2 branches were thermally grown on the Au-deposited SnO_2 nanorod stems. Samples were characterized by XRD, SEM, TEM, SAED, and PL. The branches are of single crystalline rutile SnO_2 structure. From the observation that the branch tips comprise Au-containing nanoparticles, we propose the Au-catalyzed VLS growth mechanism to mainly describe the growth process of the SnO_2 branches. The PL spectrum under excitation at 325 nm shows a broad band with a prominent emission peak around 610 nm. This method can be applied to a wide range of materials for various branched nanostructures, which may serve as potential building blocks in various advanced nanodevices.

Acknowledgement

This work was supported by Inha University Research Grant.

References

[1] Aoki A, Sasakura H. Jpn. J Appl Phys 1970;9:582.
[2] Tatsuyama C, Ichimura S. Jpn J Appl Phys 1976;15:843.
[3] Leite ER, Weber IT, Longo E, Varela JA. Adv Mater 2000;12:965.
[4] Aiyer RC, Ansari SG, Boroojerdian P, Karekar RN, Kulkarni SK, Sainkar SR. Thin Solid Films 1997;295:271.
[5] Nayral C, Viala E, Colliere V, Fau P, Senocq F, Maisonnat A, Chaudret B. Appl Surf Sci 2000;164:219.
[6] Tai WP, Oh JH. Thin Solid Films 2002;422:220.
[7] Kolmakov A, Zhang Y, Cheng G, Moskovits M. Adv Mater 2003;15:997.
[8] Dai ZR, Pan ZW, Wang ZL. Solid State Commun 2001;118:351.
[9] Wang ZL, Pan Z. Adv Mater 2002;14:1029.
[10] Liu Y, Zheng C, Wang W, Yin C, Wang G. Adv Mater 1883;2001:13.
[11] Sun SH, Meng GW, Wang YW, Gao T, Zhang MG, Tian YT, Peng XS, Zhang LD. Appl Phys A 2003;76:287.
[12] Wang D, Lieber CM. Nature Mater 2003;2:355.
[13] Satishkumar BC, Thomas PJ, Govindaraj A, Rao CNR. Appl Phys Lett 2000;77:2530.
[14] Ting JM, Chang CC. Appl Phys Lett 2002;80:324.
[15] Li J, Papadopoulos C, Xu J. Nature 1999;402:253.
[16] Kim HW, Shim SH. J Korean Phys Soc 2005;47:516.
[17] Kim HW, Kim NH, Myung JH, Shim SH. Phys Stat Sol (a) 1758;2005:202.
[18] Kim HW, Kim NH. Appl Phys A 2005;80:537.
[19] Hu JQ, Ma XL, Shang NG, Xie ZY, Wong NB, Lee CS, Lee ST. J Phys Chem B 2002; 106:3823.
[20] Cheng B, Russel JM, Shi W, Zhang L, Samulski ET. J Am Chem Soc 2004;126:5972.
[21] Hu J, Bando Y, Liu Q, Golberg D. Adv Funct Mater 2003;13:493.
[22] Maestre D, Cremades A, Piqueras J. J Appl Phys 2004;95:3027.